Vibrating Coordinates Frame Transformation Based Unity Power Factor Control of a Three-Phase Converter at Grid Voltage Imbalance and Harmonics

Sebastian Wodyk and Grzegorz Iwanski, *Senior Member, IEEE*

Abstract—**This article proposes a control system of a three-phase grid-connected power converter, operating in the rectifier mode, which achieves the unity power factor target, i.e., unbalanced and distorted current instead of sinusoidal one for grid voltage imbalance and harmonics. Such a target is known from active power filters control, but it has not been used for power supply devices yet. Thanks to that, the three-phase converter is seen as resistive load by the utility grid, and active power is consumed with minimal possible rms current, keeping current asymmetry corresponding to the voltage asymmetry during unbalanced dips. Intentional introduction of current harmonics is not trivial from the point of view of both reference signals calculation and control system structure, because in the classical approach, it would require resonant terms in controller structure. Additionally, grid voltage asymmetry introduces another oscillating component, which imposes other resonant terms in the controller. The transformation presented in this article allows to achieve desirable current harmonics and asymmetry with the use of two proportional-integral controllers, one in each controlled axis. This article presents theoretical principles of the new transformation, control system structure as well as simulation and experimental tests of a three-phase converter utilizing this idea.**

Index Terms—**AC–DC power converters, active rectifier unity power factor.**

I. INTRODUCTION

THREE-PHASE grid-connected power converters are widely used for the purpose of current rectification combined with power quality improvement functions. Although devices of this type are becoming more and more common, there are still a lot of passive rectifiers under operation, causing harmonics distortion of grid voltage. Another type of distortion that occurs in a utility grid is voltage asymmetry, caused by unbalanced load. This type of grid fault has become recently a popular research issue since it influences the control system of the three-phase power converter more than grid voltage harmonics. Devices connected to the grid should not only convert alternating current energy into direct current (dc) energy, but also support the utility grid. In near future, a new challenge for power systems may appear, which is common use of fast dc chargers for electric vehicles. Thus, supporting grid power capability and its reliability is expected of most devices, especially in the industry.

Typical control methods, such as voltage-oriented control (VOC) or direct power control (DPC), are not robust against grid voltage distortion without additional structures. In order to reduce unwanted current harmonics, phase-locked loop was introduced to keep the rotating reference frame synchronized with fundamental voltage harmonic in VOC [1]. Another approach is orientation of the rotating reference frame along the virtual flux vector [2]. Virtual flux has been found useful also in the DPC strategy [3]. However, control of grid-connected three-phase power converters under the grid harmonics condition is a less challenging issue than under grid voltage asymmetrical dips, because as long as voltage contains only the positive sequence component, its hodograph remains circular. However, if the negative sequence appears, the hodograph becomes elliptical, and hence, the grid voltage phase angle oscillates, which significantly disturbs synchronization of the rotating reference frame. Then, a double synchronous reference frame was proposed, one of which is synchronized with the positive voltage sequence component, and the second one synchronized with the negative sequence component [4], [5]. Nevertheless, due to the mutual interaction between positive and negative components, notch filters are introduced in order to eliminate double grid frequency oscillation in rotating reference frame currents, which worsens current control dynamics.

Other method is regulation of current in a stationary frame with proportional–resonant (PR) controllers [6]–[11]. Then, intentional synchronization issues are eliminated because there is no rotating reference frame, and there is no need for grid voltage phase angle determination. On the other hand, a precise current reference generator is required, which is not trivial in case of

voltage asymmetry [7], [8]. One of the targets proposed in the literature is current asymmetry opposite to voltage asymmetry. Although it allows to reduce dc-link voltage oscillations, due to the constant *p* component of instantaneous power, it is not beneficial to the grid in the rectifier operation mode, because the phase with the lowest voltage is loaded the most. Thus, researchers proposed a number of stationary frame control systems, which allow achievement of different current asymmetry, from opposite to corresponding to voltage asymmetry [9]–[12], depending on the operating mode and demanded power. One of the most problematic issues in stationary frame control systems, often omitted by the authors, is limitation of asymmetrical current. It can be done with three-phase signals based limitation structures [10]–[12].

The asymmetrical current target under grid voltage unbalanced dips has also been analyzed by the authors investigating DPC modifications [13]–[15]. Zhang *et al.* [13] proposed a deadbeat-based control system, though with a control target unbeneficial to the grid, which is current asymmetry opposite to voltage asymmetry. Another approach is utilization of proportional–integral–resonant controllers (PIR) realized as DPC structure modifications [14], [15]. Such a system allows both flexible target change and three-phase current limitation. The main disadvantage is PIR controller antiwindup realization due to simultaneous limitation of integral and resonant terms. This issue may be avoided through non-Cartesian transformation of stationary reference frame and control of current in the rotating reference frame with only two proportional-integral (PI) controllers [16]. Then, no separate negative sequence control loop and no resonant terms are needed even for the asymmetrical current target.

The support role of grid-connected converters in the field of grid voltage recovery during grid faults is more and more relevant, wherein besides frequency stabilization [17], a negative sequence voltage component minimization [18] is also of primary importance. The main feature of such a power converter is forcing, although not always symmetrical but sinusoidal, three-phase current.

Considering future challenges for the utility grid, the unity power factor target instead of sinusoidal current should be considered. Then, the converters operating in the rectifier mode are seen as a balanced resistive load by the grid. Thus, the phase with the lowest voltage is loaded the least, and active power is transferred to the dc-bus with minimum rms current values. Such a strategy was proposed for a shunt active power filter (APF) control target [19], [20]. A similar control target may be achieved with a multiple reference frame controller, then low-pass (or notch) filtering of the measured current is introduced, in order to eliminate mutual influence of positive and negative sequence components, as well as harmonics [21], which worsens control dynamics.

Moreover, designation of reference current for every reference frame is needed, which is not trivial.

Another approach is control with multioscillatory terms, which can be implemented both in stationary or rotating reference frame, though it brings further challenging issues related to controllers tuning as well as their limitation [22]. Furthermore,
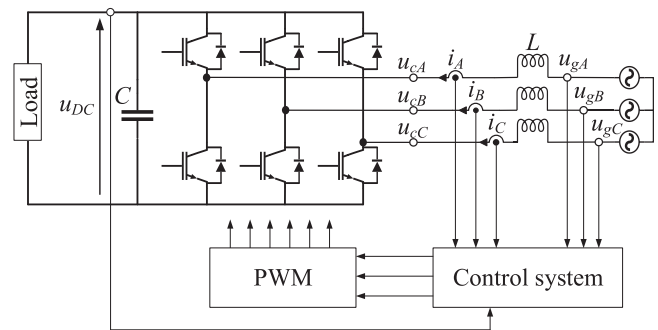

Fig. 1. Scheme of a grid-connected three-phase power converter.

appropriate current reference would still be a problem, because such systems operate usually with sinusoidal current target.

This article presents a control system of a three-phase grid-connected power converter (see Fig. 1) operating in rectifier mode, under grid voltage harmonics and asymmetry, which allows to achieve the unity power factor, so the converter is seen as a balanced resistive load by the grid. This target is achieved with two simple PI controllers, which is possible thanks to the new frame transformation.

Current limitation ensures that current in the most loaded phase does not exceed maximal allowed rms value. Nevertheless, the main contribution of this article is novel transformation, which allows to represent any $\alpha\beta$ vector containing harmonics and negative sequence component, as a nondistorted vector in the new $\alpha'\beta'$ reference frame. Moreover, a derivative-invariant inverse transformation, providing an appropriate control signal, was proposed.

II. THEORETICAL PRINCIPLES OF THE TRANSFORMATION

A. Direct Transformation

Considering three-phase signals distorted by the negative sequence component as well as fifth and seventh harmonics, they can be represented in the stationary $\alpha\beta$ reference frame as follows:

$$x_\alpha = |x_{1\alpha}| \cos(\omega t - \theta_\alpha) + |x_5| \cos(5\omega t - \theta_5)$$
$$+ |x_7| \cos(7\omega t - \theta_7) \tag{1}$$
$$x_\beta = |x_{1\beta}| \sin(\omega t - \theta_\beta) - |x_5| \sin(5\omega t - \theta_5)$$
$$+ |x_7| \sin(7\omega t - \theta_7) \tag{2}$$

where $|x_{1\alpha}|$ and $|x_{1\beta}|$ are amplitudes of fundamental harmonic $\alpha\beta$ components, $|x_5|$ and $|x_7|$ are amplitudes of fifth and seventh harmonics, θ_α and θ_β are phase shifts between the corresponding component and positive sequence component, and θ_5 and θ_7 are phase shifts between corresponding harmonic and fundamental harmonic positive sequence component.

The purpose of the proposed transformation is representation of variables, which are distorted in the $\alpha\beta$ stationary frame, by nondistorted, orthogonal components in a new $\alpha'\beta'$ reference

frame. In this new reference frame, original signals are represented in the following manner:

$$\begin{bmatrix} x'_\alpha \\ x'_\beta \end{bmatrix} = \begin{bmatrix} X_{\text{base}} \cos(\omega t) \\ X_{\text{base}} \sin(\omega t) \end{bmatrix} \tag{3}$$

where X_{base} is the length of the new $x'_{\alpha\beta}$ vector.

The transformation from $\alpha\beta$ to $\alpha'\beta'$ reference frame is described by matrix T, which is presented in (4), the dimension of which is two by two. It means that four independent coefficients need to be determined

$$\begin{bmatrix} x'_\alpha \\ x'_\beta \end{bmatrix} = T \begin{bmatrix} x_\alpha \\ x_\beta \end{bmatrix} \tag{4}$$

where

$$T = \begin{bmatrix} t_{11} & t_{12} \\ t_{21} & t_{22} \end{bmatrix}. \tag{5}$$

Due to occurrence of fifth and seventh harmonics and asymmetry, the $\alpha'\beta'$ frame is not orthogonal or stationary. The original hodograph takes the form of a superposition of an ellipse, representing fundamental harmonic and high harmonics, which makes a full circle a certain number of times per fundamental period. Seeing that four unknowns need to be determined, a system of four equations is required, whereas dependence between $\alpha'\beta'$ and $\alpha\beta$ components gives only two equations. It can be assumed that any phase shift of the whole original signal results in the corresponding phase shift in the transformed signal. A particular case of such a phase shift is signal delayed by $\pi/2$. The original signal in the $\alpha\beta$ reference frame delayed by $\pi/2$ is described as follows:

$$x_\alpha^q = |x_{1\alpha}| \sin(\omega t - \theta_\alpha) + |x_5| \sin(5\omega t - \theta_5)$$
$$- |x_7| \sin(7\omega t - \theta_7) \tag{6}$$
$$x_\beta^q = -|x_{1\beta}| \cos(\omega t - \theta_\beta) + |x_5| \cos(5\omega t - \theta_5)$$
$$+ |x_7| \cos(7\omega t - \theta_7). \tag{7}$$

Accordingly, components in the $\alpha'\beta'$ frame take the form

$$\begin{bmatrix} x_\alpha'^q \\ x_\beta'^q \end{bmatrix} = \begin{bmatrix} X_{\text{base}} \sin(\omega t) \\ -X_{\text{base}} \cos(\omega t) \end{bmatrix}. \tag{8}$$

The transformation from $\alpha\beta$ to $\alpha'\beta'$ frames for the phase-shifted signals is also described by matrix T, which gives two other equations, and as a result, the following system of four equations may be created:

$$\begin{bmatrix} x'_\alpha \\ x'_\beta \\ x_\alpha'^q \\ x_\beta'^q \end{bmatrix} = \begin{bmatrix} t_{11}x_\alpha + t_{12}x_\beta \\ t_{21}x_\alpha + t_{22}x_\beta \\ t_{11}x_\alpha^q + t_{12}x_\beta^q \\ t_{21}x_\alpha^q + t_{22}x_\beta^q \end{bmatrix}. \tag{9}$$

By solving the equations, matrix T coefficients are obtained and take the following form:

$$T =$$

$$\frac{X_{\text{base}}}{|x_p|\,d} \begin{bmatrix} x_{p\alpha}\left(x_{5\alpha} - x_{7\alpha} - x_{1\beta}^q\right) - x_{p\beta}\left(x_{1\beta} + x_{5\beta} + x_{7\beta}\right) \\ x_{p\alpha}\left(x_{1\beta} + x_{5\beta} + x_{7\beta}\right) + x_{p\beta}\left(x_{5\alpha} + x_{7\alpha} + x_{1\beta}^q\right) \end{bmatrix}$$
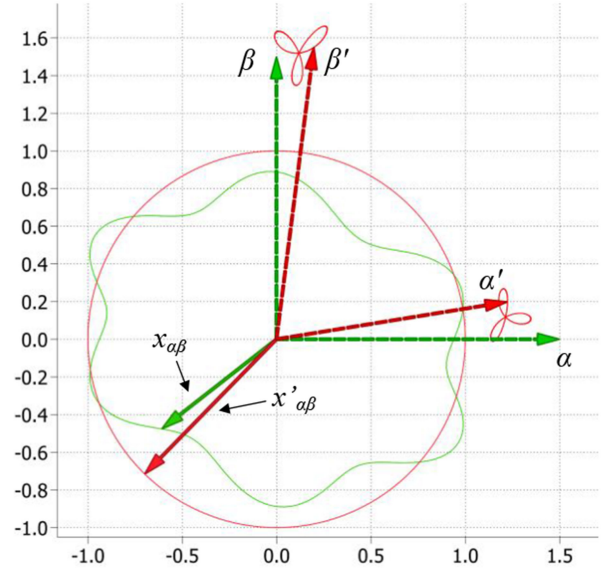

Fig. 2. Vector $x_{\alpha\beta}$ containing fifth and seventh harmonic and negative sequence component and its representation in the new $\alpha'\beta'$ reference frame.

$$\begin{matrix} x_{p\alpha}\left(x_{5\beta} + x_{7\beta} - x_{1\alpha}^q\right) + x_{p\beta}\left(x_{1\alpha} + x_{5\alpha} + x_{7\alpha}\right) \\ -x_{p\alpha}\left(x_{1\alpha} + x_{5\alpha} + x_{7\alpha}\right) + x_{p\beta}\left(x_{5\beta} + x_{7\beta} - x_{1\alpha}^q\right) \end{matrix} \tag{10}$$

where

$$d = |x_5|^2 + |x_7|^2 + x_{1\beta}\left(x_{5\beta} + x_{7\beta} - x_{1\alpha}^q\right)$$
$$+ x_{1\alpha}\left(x_{5\alpha} + x_{7\alpha} + x_{1\beta}^q\right) + 2x_{5\alpha}x_{7\alpha} - x_{5\beta}x_{1\alpha}^q$$
$$+ x_{5\alpha}x_{1\beta}^q - x_{7\beta}x_{1\alpha}^q + x_{7\alpha}x_{1\beta}^q. \tag{11}$$

Axes of a new $\alpha'\beta'$ frame are not only shifted with respect to the original axes due to asymmetry, but also hesitate around this shift, so the new reference frame is no longer stationary, which can be seen in Fig. 2.

B. Inverse Transformation

In order to make the proposed transformation useful in the context of converter control, an inverse transformation needs to be determined. It is natural that inversion of matrix T may be considered first, though this option is far from the right solution, because it does not take into account the physics of the plant, which is grid filter. For the inductive filters, the control system, considering grid voltage feedforward, is generally responsible for providing proper filter voltage drop. It is known that this voltage drop is proportional to the time derivative of current and the inductance value $u_L = L\,di/dt$. Due to that, while forced current contains harmonics, a new transformation based on derivatives of original signals needs to be utilized, which is described as follows:

$$\frac{d}{dt}\begin{bmatrix} x_\alpha \\ x_\beta \end{bmatrix} = T_{\text{inv}} \frac{d}{dt}\begin{bmatrix} x'_\alpha \\ x'_\beta \end{bmatrix} \tag{12}$$

where

$$T_{\text{inv}} \neq T^{-1} \tag{13}$$

$$\mathrm{T_{inv}} = \begin{bmatrix} t_{11_{inv}} & t_{12_{inv}} \\ t_{21_{inv}} & t_{22_{inv}} \end{bmatrix}. \tag{14}$$

The mentioned derivatives are described in the following way:

$$\frac{d}{dt}x_\alpha = \omega(-|x_{1\alpha}|\sin(\omega t - \theta_\alpha)$$
$$- 5|x_5|\sin(5\omega t - \theta_5) - 7|x_7|\sin(7\omega t - \theta_7)) \tag{15}$$

$$\frac{d}{dt}x_\beta = \omega(|x_{1\beta}|\cos(\omega t - \theta_\beta)$$
$$- 5|x_5|\cos(5\omega t - \theta_5) + 7|x_7|\cos(7\omega t - \theta_7)) \tag{16}$$

$$\frac{d}{dt}x'_\alpha = -\omega X_{base}\sin(\omega t) \tag{17}$$

$$\frac{d}{dt}x'_\beta = \omega X_{base}\cos(\omega t) \tag{18}$$

and their quadrature components

$$\frac{d}{dt}x^q_\alpha = \omega(|x_{1\alpha}|\cos(\omega t - \theta_\alpha)$$
$$+ 5|x_5|\cos(5\omega t - \theta_5) + 7|x_7|\cos(7\omega t - \theta_7)) \tag{19}$$

$$\frac{d}{dt}x^q_\beta = \omega(|x_{1\beta}|\sin(\omega t - \theta_\beta)$$
$$- 5|x_5|\sin(5\omega t - \theta_5) - 7|x_7|\sin(7\omega t - \theta_7)) \tag{20}$$

$$\frac{d}{dt}{x'_\alpha}^q = \omega X_{base}\cos(\omega t) \tag{21}$$

$$\frac{d}{dt}{x'_\beta}^q = \omega X_{base}\sin(\omega t). \tag{22}$$

An inverse transformation matrix can be derived, such as the direct transformation matrix, and as a result is described as

$$\mathrm{T_{inv}} = \frac{1}{X_{base}|x_p|}$$

$$\begin{bmatrix} x_{p\alpha}(x_{1\alpha} + 5x_{5\alpha} - 7x_{7\alpha}) + x_{p\beta}(-5x_{5\beta} + 7x_{7\beta} + x^q_{1\alpha}) \\ x_{p\alpha}(x_{1\beta} + 5x_{5\beta} - 7x_{7\beta}) + x_{p\beta}(5x_{5\alpha} - 7x_{7\alpha} + x^q_{1\beta}) \end{bmatrix}$$

$$\left. \begin{matrix} x_{p\alpha}(5x_{5\beta} - 7x_{7\beta} - x^q_{1\alpha}) + x_{p\beta}(x_{1\alpha} + 5x_{5\alpha} - 7x_{7\alpha}) \\ -x_{p\alpha}\left(5x_{5\alpha} - 7x_{7\alpha} + x^q_{1\beta}\right) + x_{p\beta}(x_{1\beta} + 5x_{5\beta} - 7x_{7\beta}) \end{matrix} \right].$$
$$\tag{23}$$

The presented transformation takes into account only fifth and seventh harmonic, but it can be simply extended to any number of harmonic which occurs in three wire systems. General form of direct and inverse transformation, as well as their derivation is presented in the Appendix.

C. Direct and Inverse Transformation Parameters

In order to calculate matrices T and T_{inv} coefficients, some components of the original signal need to be extracted. They are fundamental harmonic $x_{1\alpha\beta}$ and its quadrature component $x^q_{1\alpha\beta}$, fifth and seventh harmonics $x_{5\alpha\beta}$, $x_{7\alpha\beta}$, and positive sequence
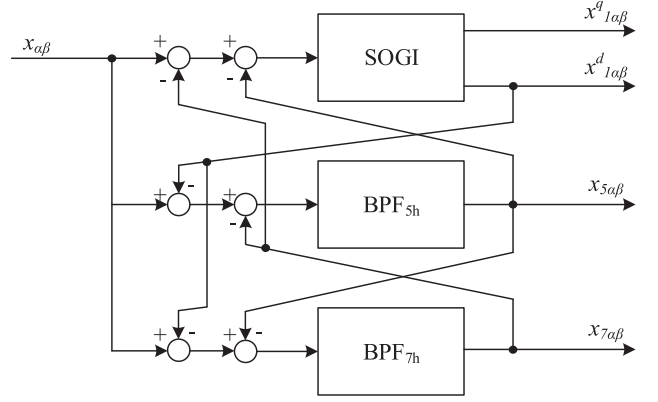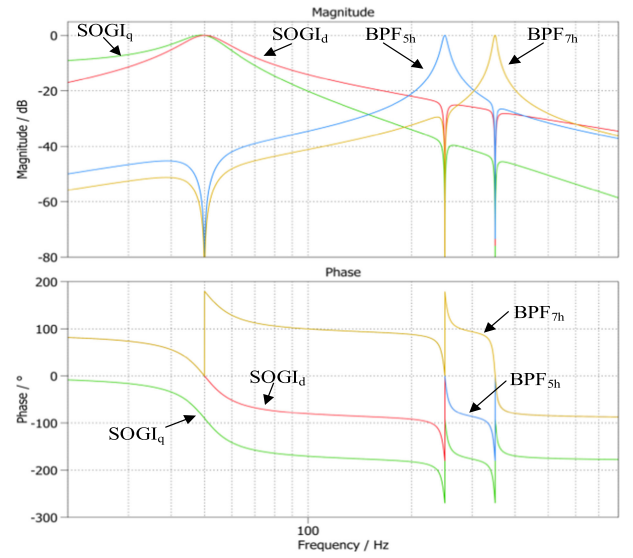

Fig. 3.   Feedback-based filtration structure.

Fig. 4.   Bode plots of the feedback-based filters.

component $x_{p\alpha\beta}$. These parameters may be achieved with adequate filtration. For fundamental harmonic and its quadrature component, the second-order generalized integrator may be utilized [23], whereas for the fifth and seventh harmonics, bandpass filtration may be used. In order to reduce mutual share of each component in the desired signals, a novel filtration structure using filters feedback is proposed. This structure is presented in Fig. 3. A greater attenuation for unwanted frequencies in each filtration path is achieved, and there is no need for increasing the order of the filter, which would result in higher computational burden, or to narrow the bandwidth of the low-order filters, which causes poor dynamics. Feedback-based filtration provides good dynamics of low-order filtration by keeping a wide bandwidth and cutting out unwanted frequencies.

Bode plots of the discussed filters are shown in Fig. 4, obtained for parameters presented in Table I. It is clearly visible that frequencies that are naturally contained in input signal are strongly damped by filters. Furthermore, the positive sequence component needs to be calculated, it can be done with the

TABLE I
PARAMETERS OF FILTERS USED IN FEEDBACK-BASED STRUCTURE

SYMBOL	TRANSFER FUNCTION	PARAMETER
BPF$_{5h}$	$G(s) = \dfrac{Bs}{s^2 + Bs + \omega_0^2}$	$\omega_0 = 500\pi$ $B = 20\pi$
BPF$_{7h}$	$G(s) = \dfrac{Bs}{s^2 + Bs + \omega_0^2}$	$\omega_0 = 700\pi$ $B = 20\pi$
SOGI	$G_d(s) = \dfrac{k\omega_0 s}{s^2 + k\omega_0 s + \omega_0^2}$ $G_q(s) = \dfrac{k\omega_0^2}{s^2 + k\omega_0 s + \omega_0^2}$	$\omega_0 = 100\pi$ $k = 0.3$

following equations:

$$x_{p\alpha} = \frac{x_{1\alpha} - x_{1\beta}^q}{2} \tag{24}$$

$$x_{p\beta} = \frac{x_{1\beta} + x_{1\alpha}^q}{2} . \tag{25}$$

Another issue is correct selection of X_{base}, which is representation of a new $x'_{\alpha\beta}$ vector magnitude. Considering the three-phase power converter current control, limitation of the current rms value should be taken into account, because of conduction losses in power switches. An ordinary approach, the goal of which is keeping symmetrical sinusoidal current, allows to simplify this issue to vector magnitude limitation. This problem becomes more complex for asymmetrical sags, where keeping the asymmetrical current is the goal, because the current vector in the $\alpha\beta$ frame takes an elliptical form, and its magnitude varies in time. Some strategies allowing asymmetrical three-phase current limitation were proposed in the literature [11], [12], [15], nevertheless the limitation level is still intuitive due to constant relation of the sinusoidal signal amplitude to its rms vale, that equals $\sqrt{2}$. Considering that the converter is seen by the grid as a balanced resistive load, the highest rms current values are achieved in the phase with the highest rms voltage value. Assuming that $X_{\text{base}} = \max\{x_{A\text{rms}}, x_{B\text{rms}}, x_{C\text{rms}}\}$, the vector $x'_{\alpha\beta}$ magnitude refers to the greatest rms value among the three-phase signals. Calculation of the three-phase signals rms values, considering fifth and seventh harmonics, may be done with

$$x_{\text{rms}} = \sqrt{\frac{|x_1|^2 + |x_5|^2 + |x_7|^2}{2}}. \tag{26}$$

As vector magnitude in the standard $\alpha\beta$ frame for nondistorted signals refers to the amplitude of three-phase signals, a better approach is to use the amplitude of the theoretical fundamental harmonic component created by multiplying the rms value by $\sqrt{2}$. Then, X_{base} selection may be described with the following formula:

$$X_{\text{base}} = \max\{ \sqrt{|x_{1A}|^2 + |x_5|^2 + |x_7|^2},$$

$$\sqrt{|x_{1B}|^2 + |x_5|^2 + |x_7|^2},$$

$$\sqrt{|x_{1C}|^2 + |x_5|^2 + |x_7|^2}\}. \tag{27}$$

Amplitudes of fundamental harmonics may be calculated in the following way:

$$|x_{1A}| = \sqrt{x_{1\alpha}^2 + x_{1\alpha}^{q\,2}} \tag{28}$$

$$|x_{1B}| = \frac{1}{2}\sqrt{\left(x_{1\alpha} + \sqrt{3}x_{1\beta}\right)^2 + \left(x_{1\alpha}^q + \sqrt{3}x_{1\beta}^q\right)^2} \tag{29}$$

$$|x_{1C}| = \frac{1}{2}\sqrt{\left(x_{1\alpha} - \sqrt{3}x_{1\beta}\right)^2 + \left(x_{1\alpha}^q - \sqrt{3}x_{1\beta}^q\right)^2} . \tag{30}$$

III. PRACTICAL IMPLEMENTATION OF THE TRANSFORMATION

Achieving current that contains intentionally forced harmonics is not trivial for the grid-connected three-phase power converter. First of all, reference of these harmonics is problematic, although the control system is also difficult to design, assuming a classical VOC approach. Resonant terms in current controllers are needed, in order to achieve the zero steady-state error. Additionally, in the case of voltage asymmetry, the control system becomes more complex. The main purpose of the presented transformation application is to simplify the control system of three-phase converters operating in rectifier mode, with the unity power factor target. Then, converter current takes the shape of grid voltage. The unity power factor approach, which means load is seen as pure resistance by the grid, has been proposed as an APF control strategy. Nunez-Zuniga and Pomilio [19] and Castellan et al. [20] indicate two main advantages of such an approach. The first one is capability of possible resonance damping, which may occur for grid voltage harmonics.

If sinusoidal load current is forced, there is an open circuit from the harmonics source point of view. As resonant circuits are common in the utility grid, due to line inductance and capacitance, lack of damping may lead to amplification of certain harmonics, and in the worst case to appearance of dangerous voltage value. Another advantage is the unity power factor, which means that active power is transferred to a load with minimum rms current and minimum apparent power, which allows minimization of transmission system losses, and from the point of view of the converter, conduction losses in power switches.

A control system using the proposed transformation is presented in Fig. 5. Transformation matrices T and T_{inv} parameters are calculated with the grid voltage u_g vector in the $\alpha\beta$ stationary frame, decomposed to the required components. Such a transformation is used then to achieve the current i vector in the new $\alpha'\beta'$ frame, in which it has a constant magnitude and rotates synchronously with the grid voltage positive component. Then, the rotating dq reference frame transformation may be done, and current is represented as dc values. No additional harmonic reference is needed, because transformation is responsible for their occurrence. Current is controlled with PI controllers, such as in classical VOC, with voltage positive sequence component phase angle. Current in the d'-axis is responsible for active power
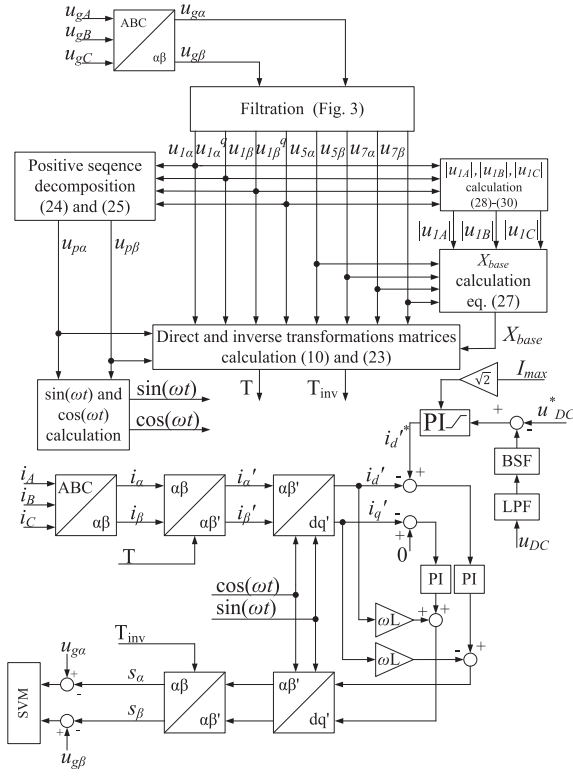
Fig. 5. Block scheme of the proposed control system.

Fig. 6. Example of the proposed control system operation, $i_{\alpha\beta}$—converter current in the stationary $\alpha\beta$ reference frame, $i_{\alpha\beta}'$—converter current in the new $\alpha'\beta'$ reference frame, i_{dq}'—converter current in the rotating $d'q'$ reference frame, current controllers output signals, $s_{\alpha\beta}$—control signal before feedforward.

TABLE II
PARAMETERS OF A SIMULATED CIRCUIT AND LABORATORY RIG

SYMBOL	QUANTITY	VALUE
U_{gn}	Nominal grid voltage (L-L rms)	230 V
I_{max}	Maximal rms current	10 A
L	Grid filter inductance	2.5 mH
R_L	Inductor resistance	40 mΩ
C_{DC}	DC-link capacitance	0.5 mF
U_{DC}	Reference DC voltage	390 V
f_s	Switching frequency	10 kHz

TABLE III
PARAMETERS OF DC-LINK VOLTAGE FILTERS

SYMBOL	TRANSFER FUNCTION	PARAMETER
LPF	$G(s) = \dfrac{\omega_0^2}{s^2 + \omega_0 s + \omega_0^2}$	$\omega_0 = 300\pi$
BSF	$(s) = \dfrac{s^2 + \omega_0^2}{s^2 + \omega_c s + \omega_0^2}$	$\omega_0 = 200\pi$ $\omega_c = 20\pi$

supply to the dc-bus, thus its reference is given by a dc voltage controller. Since the target is the unity power factor, the q'-axis current reference is equal to zero. Such a strategy allows to achieve the assumed goal, which is current that contains the same harmonics as grid voltage and keeping the same asymmetry.

The value of i_d' is related to the rms of current in the phase of the greatest rms voltage value (and therefore, the greatest rms current value) multiplied by $\sqrt{2}$. Limitation of i_d' allows to limit maximal acceptable rms current, keeping the control target. Voltage in the dc-link contains oscillations caused by grid voltage and current asymmetry and harmonics, so additional filtration is introduced, in order to reduce the influence of these oscillations on the reference current. Fig. 6 presents exemplary results for arbitrary current reference, for the purpose of illustration of control system principles.

Transformation to the $\alpha'\beta'$ reference frame results in symmetrical sinusoidal signals of a new current vector, which afterward is transformed to the rotating $d'q'$ reference frame, and takes the form of dc values, so PI controllers are sufficient to achieve the control target. Finally, the control signal is transformed back to the stationary $\alpha\beta$ reference frame (see $s_{\alpha\beta}$ in Fig. 6). This signal contains a visibly higher content of harmonics than the stationary frame current vector. The reason for this phenomenon has been explained in Section II-B.

IV. SIMULATION AND EXPERIMENTAL RESULTS

Simulation and experimental tests were conducted with two-level converter, built with three IGBT half-bridge modules. The dc load has been simulated with current source, whereas in
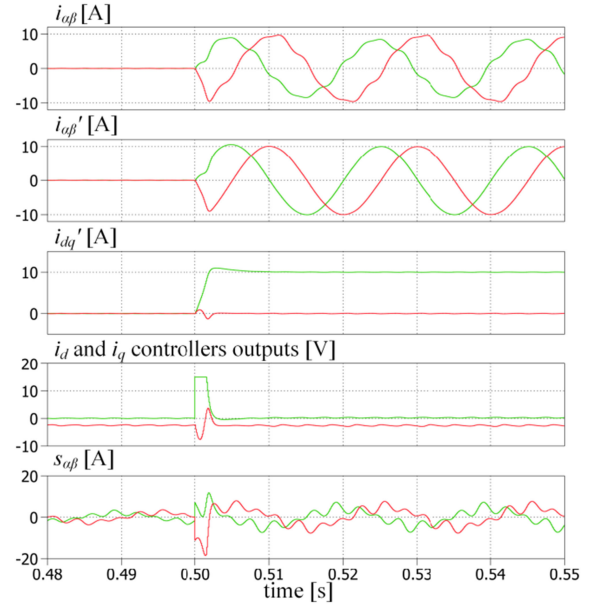
the experiment, another three-phase converter is used as a dc load. Both main and load converters were controlled with a DSP controller built with TMS320F28335. The parameters of the tested circuit are shown in Table II.

The control system contained the filtration structure presented in Fig. 3 with parameters from Table I. Parameters of an additional filtration of dc-link voltage are presented in Table III.
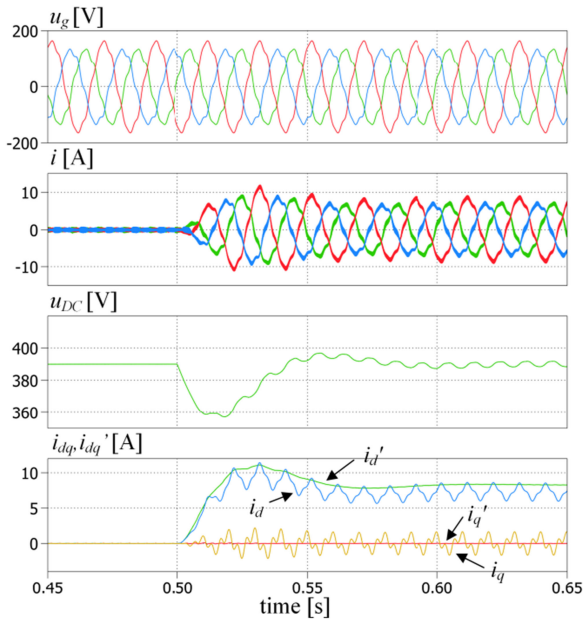
Fig. 7. Simulation results presenting step change of the dc load, grid voltage u_g, converter current i, dc-link voltage u_{DC}, current in the rotating reference frame synchronized with the grid voltage positive sequence component derived from the proposed transformation i_d', i_q', and from the classical transformation i_d, i_q.

Fig. 8. Simulation results presenting comparison of the proposed method with multioscillatory controllers and multiple reference frame control.

Tests were conducted for a two-phase voltage dip. Simulated voltage rms values are 93, 113, and 93 V, respectively, whereas the amplitudes of fifth and seventh harmonics equal 7 V. Fig. 7 presents simulation of a step change of dc load. Converter current takes the demanded shape in case of dc-bus voltage regulation. As can be noticed, dc voltage is oscillating, which can influence the reference current $i_d'^*$ value, and in consequence, the control target may be difficult to achieve. On the other hand, stronger dc voltage filters may be applied, which decreases dynamics. Thus, appropriate tradeoff between dynamics and precision of the current shape should be found, depending on application.

Comparison of new current vector components i_d', i_q' in the rotating reference frame to ordinary i_d, i_q is also presented. Both vectors are calculated for the frame synchronized with the grid voltage positive sequence component. It can be seen that ordinary vector components are strongly distorted due to asymmetry and harmonics.

In order to achieve the presented control target in a rotating reference frame derived from the classical stationary frame, those oscillations need to be designated and added to the reference i_d average value, responsible for active power transfer, which is not trivial. Moreover, it should be noted that such an analysis is simplified because reference oscillations coming from harmonics should be designated separately for positive and negative sequence components of the current vector, and applied in the double-synchronous reference frame system in order to achieve the required current asymmetry.

Alternatively, every current component can be controlled independently with a multiple reference frame [23], oriented along accordingly grid voltage positive and negative sequence components, as well as fifth and seventh harmonics, which
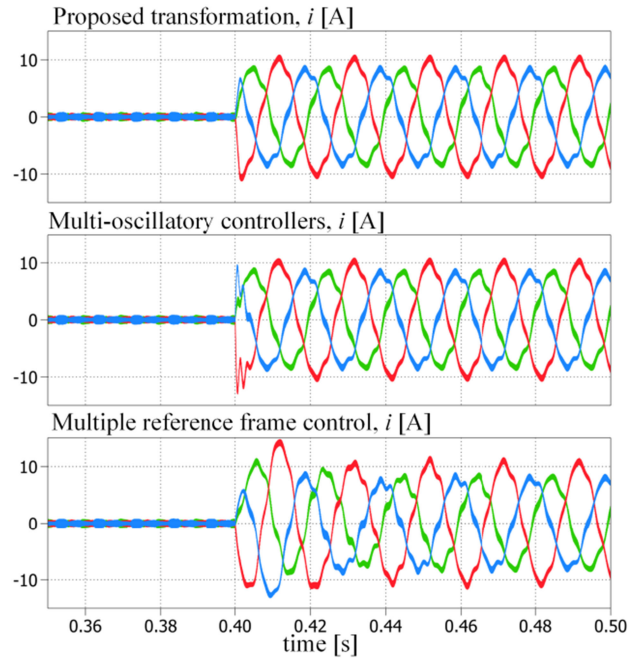
stands for four reference frames and, hence, eight PI controllers. Another approach is control in stationary frame, with the use of PR controllers with multioscillatory terms [22] for 50, 250, and 350 Hz. Fig. 8. presents comparison of the mentioned methods with the proposed one for step change of the reference current.

Definitely the worst results are given by a multireference frame, which means visibly higher overshoot and long settling time due to introduction of filters in the control loop. Multioscillatory-based control brings better results, which are comparable with the proposed method. Nevertheless, this case requires tuning of three terms of controllers, as well as introduction of a sophisticated antiwindup method.

Fig. 9 presents grid voltage u_g and converter current i steady-state waveforms and their fast Fourier transform (FFT). Noticeably, current fifth and seventh harmonics imitate grid voltage harmonics with good precision.

The experiment was conducted using the setup presented in Fig. 10. Results were recorded with a DL850E Scopecorder. Three-phase current measurement was realized with an A622 probe with 100-kHz bandwidth. New $d'q'$ current components were obtained from the control unit using a digital-to-analogue converter built in the controller board.

Experimental results for step change of the dc load are presented in Fig. 11. As can be seen, results are similar to simulation, which confirms the correctness of the control system implementation and its practical usefulness. Current components in the new $d'q'$ reference frame are slightly distorted, which is caused by some factors omitted in simulation, such as measuring noise, deadtime (2.5 μs) applied in the laboratory converter, imprecise grid voltage feedforward due to delays caused by signal processing (100 μs), or grid filter inductor resistance (see
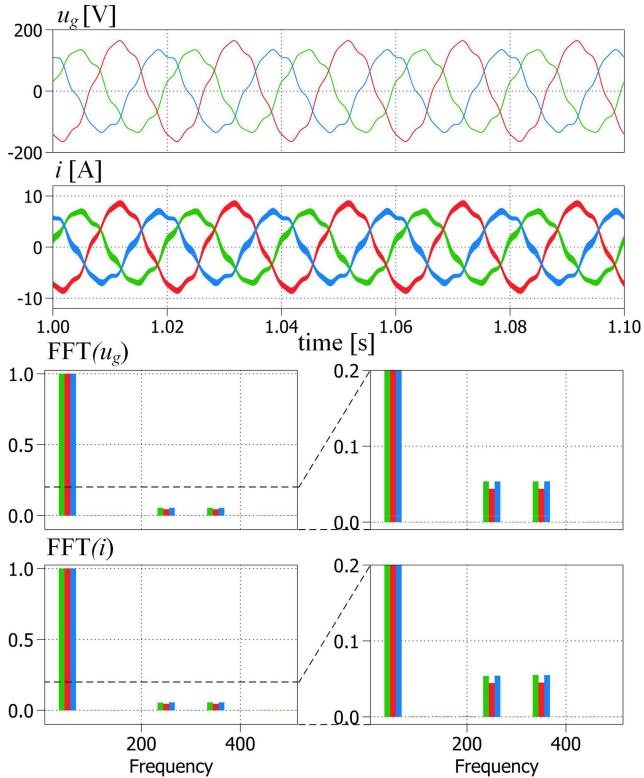
Fig. 9. Oscillograms presenting simulated grid voltage u_g and converter current i and their FFT in relation to fundamental harmonic for each phase.
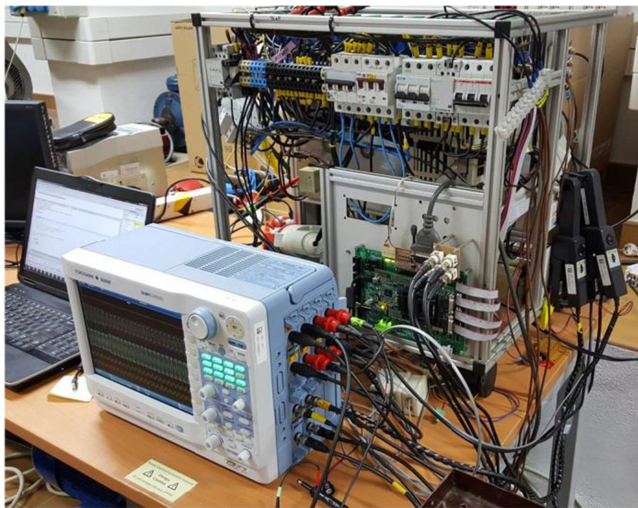

Fig. 10. Laboratory setup of a three-phase grid-connected converter used in the experiment.

Table III). However, they do not significantly disturb operation of the control system.

Fig. 12 presents a two-phase grid voltage dip during constant load of dc-bus. Converter current takes the required shape in some time after the distortion occurred. This time depends on the applied filters parameter as well as current controllers. Current reference $i_d'^*$ changes because it refers to the phase with the
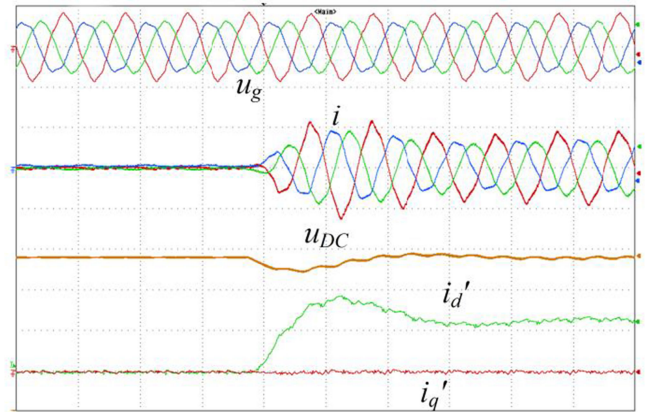

Fig. 11. Experimental results presenting step change of the dc load, grid voltage u_g (200 V/div), converter current i (10 A/div), dc-link voltage u_{DC} (100 V/div), and current in the rotating reference frame synchronized with grid voltage positive sequence component derived from the proposed transformation i_d', i_q' (6 A/div).
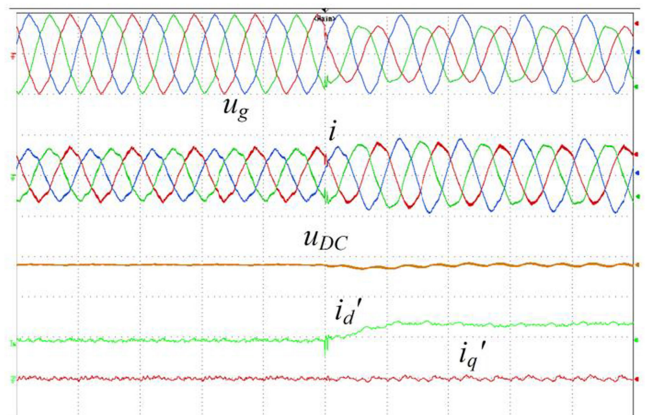

Fig. 12. Experimental results presenting an asymmetrical grid voltage dip for constant dc load, grid voltage u_g (200 V/div), converter current i (10 A/div), dc-link voltage u_{DC} (100 V/div), and current in rotating reference frame synchronized with grid voltage positive sequence component derived from the proposed transformation i_d', i_q' (6 A/div).

TABLE IV
POWER FACTOR IN EACH PHASE

CASE	PF_A	PF_B	PF_C
Symmetrical grid voltage	0.998	0.998	0.999
Two-phase grid voltage dip	0.998	0.998	0.998

greatest rms value. As the active power demand did not change, current needs to be higher because of the voltage dip, therefore i_d' rises.

Based on grid voltage and current oscillograms presented in Fig. 12, the power factor for each phase has been calculated, according to the formula

$$\text{PF} = \frac{P}{S} = \frac{\frac{1}{T}\int_t^{t+T} u(t)\,i(t)\,dt}{\sqrt{\frac{1}{T}\int_t^{t+T} u^2(t)\,dt \int_t^{t+T} i^2(t)\,dt}} \quad (31)$$

where $T = 20$ ms. The results are presented in Table IV. It can be seen that power factor PF keeps a high value (≥ 0.99) even in case of grid voltage asymmetry, which confirms the assumptions.

V. CONCLUSION

This article presented an innovative approach to grid-connected three-phase power converters control, which was keeping the unity power factor instead of sinusoidal current using novel transformation of signals from the stationary reference frame to the new frame in which unbalanced and distorted three-phase signals were represented as balanced and sinusoidal signals, so after further Park's transformation, the signals became constant. Intentionally introduced current harmonics and asymmetry were achieved with well-known PI controllers. No resonant terms for 6ω (coming from fifth and seventh harmonics) as well as for 2ω (coming from asymmetry) were needed. Direct and inverse transformations were described by matrices, the parameters of which were calculated on the basis of grid voltage components in the $\alpha\beta$ stationary frame, which were provided by the feedback-based filtration structure. Thanks to that, good attenuation of unwanted frequencies was achieved, maintaining satisfactory dynamics. Signals obtained from the filtration structure were directly used in the new transformation, thus no additional calculations requiring high computational burden (such as, e.g., trigonometric functions) were needed. Thus, the whole structure was easy to complete with digital-signal processors, common in industry, such as the used TMS320F28335, which was a typical industrial microcontroller.

Control systems with dc-link voltage regulation were tested during both simulation and experimental tests, which confirmed the correctness of the assumptions. The obtained results gave, with a negligible error, the true unity power factor, i.e., the content of negative sequence and harmonics components in the converter current, the same as in the grid voltage.

A further extension of the transformation for higher harmonics order was possible, but the possible range of harmonics that can be taken into account strictly depends on the sampling frequency due to the limited precision of digital filters for the frequencies comparable to the sampling frequencies. However, it was common also for other methods.

APPENDIX

Derivation of the General Transformation

In general, original vector components may be described as in (31) and (32)

$$x_\alpha = x_{1\alpha} + K_\alpha + M_\alpha \tag{32}$$

$$x_\beta = x_{1\beta} + K_\beta + M_\beta \tag{33}$$

$$x_\alpha^q = x_{1\alpha}^q - K_\beta + M_\beta \tag{34}$$

$$x_\beta^q = x_{1\beta}^q + K_\alpha - M_\alpha \tag{35}$$

where

$$K_\alpha = \sum_{n=1}^{\infty} \left(x_{(12n-7)\alpha} + x_{(12n-5)\alpha} \right) \tag{36}$$

$$K_\beta = \sum_{n=1}^{\infty} \left(x_{(12n-7)\beta} + x_{(12n-5)\beta} \right) \tag{37}$$

$$M_\alpha = \sum_{n=1}^{\infty} \left(x_{(12n-1)\alpha} + x_{+(12n+1)\alpha} \right) \tag{38}$$

$$M_\beta = \sum_{n=1}^{\infty} \left(x_{(12n-1)\beta} + x_{+(12n+1)\beta} \right) \tag{39}$$

Then direct transformation matrix T takes the form:

$$\mathrm{T} = \frac{X_{base}}{|x_p|d} \begin{bmatrix} x_{p\alpha} \left(x_{1\beta}^q + K_\alpha - M_\alpha \right) - x_{p\beta} \left(x_{1\beta} + K_\beta + M_\beta \right) \\ x_{p\alpha} \left(x_{1\beta} + K_\beta + M_\beta \right) + x_{p\beta} \left(x_{1\beta}^q + K_\alpha - M_\alpha \right) \\ -x_{p\alpha} \left(x_{1\alpha}^q - K_\beta + M_\beta \right) + x_{p\beta} \left(x_{1\alpha} + K_\alpha + M_\alpha \right) \\ -x_{p\alpha} \left(x_{1\alpha} + K_\alpha + M_\alpha \right) - x_{p\beta} \left(x_{1\alpha}^q - K_\beta + M_\beta \right) \end{bmatrix} \tag{40}$$

where

$$d = x_{1\alpha} (K_\alpha - M_\alpha) + x_{1\beta}^q (K_\alpha + M_\alpha) - x_{1\alpha}^q (K_\beta + M_\beta)$$
$$+ x_{1\beta} (K_\beta - M_\beta) + K_\alpha^2 + K_\beta^2 - M_\alpha^2 + M_\beta^2$$
$$+ x_{1\alpha} x_{1\beta}^q - x_{1\alpha}^q x_{1\beta} \tag{41}$$

What can be further simplified:

$$\mathrm{T} = \frac{X_{base}}{|x_p|(x_\alpha x_\beta^q - x_\alpha^q x_\beta)} \begin{bmatrix} x_{p\alpha} x_\beta^q - x_{p\beta} x_\beta & -x_{p\alpha} x_\alpha^q + x_{p\beta} x_\alpha \\ x_{p\alpha} x_\beta + x_{p\beta} x_\beta^q & -x_{p\alpha} x_\alpha - x_{p\beta} x_\alpha^q \end{bmatrix} \tag{42}$$

Analogously, general inverse transformation may be derived in the following way:

$$\frac{d}{dt} x_\alpha = \omega \left(-x_{1\alpha}^\alpha + D_\beta - H_\beta \right) \tag{43}$$

$$\frac{d}{dt} x_\beta = \omega \left(-x_{1\beta}^\alpha - D_\alpha + H_\alpha \right) \tag{44}$$

$$\frac{d}{dt} x_\alpha^q = \omega (x_{1\alpha} + L_\alpha - N_\alpha) \tag{45}$$

$$\frac{d}{dt} x_\beta^q = \omega (x_{1\beta} + L_\beta - N_\beta) \tag{46}$$

where:

$$D_\alpha = \sum_{n=1}^{\infty} \left((12n - 7)x_{(12n-7)\alpha} + (12n - 1)x_{(12n-1)\alpha} \right) \tag{47}$$

$$D_\beta = \sum_{n=1}^{\infty} \left((12n - 7)x_{(12n-7)\beta} + (12n - 1)x_{(12n-1)\beta} \right) \tag{48}$$

$$H_\alpha = \sum_{n=1}^{\infty} \left((12n - 5)x_{(12n-5)\alpha} + (12n + 1)x_{(12n+1)\alpha} \right) \tag{49}$$

$$H_\beta = \sum_{n=1}^{\infty} \left((12n - 5)x_{(12n-5)\beta} + (12n + 1)x_{(12n+1)\beta} \right) \tag{50}$$

$$L_\alpha = \sum_{n=1}^{\infty} \left((12n - 7)x_{(12n-7)\alpha} - (12n - 5)x_{(12n-5)\alpha} \right) \tag{51}$$

$$L_\beta = \sum_{n=1}^{\infty} \left((12n - 7)x_{(12n-7)\beta} - (12n - 5)x_{(12n-5)\beta} \right) \tag{52}$$

$$N_\alpha = \sum_{n=1}^{\infty} \left((12n - 1)x_{(12n-1)\alpha} - (12n + 1)x_{(12n+1)\alpha} \right) \tag{53}$$

$$N_\beta = \sum_{n=1}^{\infty} \left((12n-1)x_{(12n-1)\beta} - (12n+1)x_{(12n+1)\beta} \right) \tag{54}$$

$$\mathbf{T}_{inv} = \frac{1}{X_{base|x_p|}} \begin{bmatrix} x_{p\alpha}(x_{1\alpha}+L_\alpha-N_\alpha) - x_{p\beta}(-x_{1\alpha}^q + D_\beta - H_\beta) \\ x_{p\alpha}(x_{1\beta}+L_\beta-N_\beta) - x_{p\beta}(-x_{1\beta}^q - D_\alpha + H_\alpha) \end{bmatrix}$$

$$\left. \begin{matrix} x_{p\alpha}(-x_{1\alpha}^q + D_\beta - H_\beta) + x_{p\beta}(x_{1\alpha}+L_\alpha-N_\alpha) \\ x_{p\alpha}(-x_{1\alpha}^q + D_\beta - H_\beta) + x_{p\beta}(x_{1\beta}+L_\beta-N_\beta) \end{matrix} \right] \tag{55}$$

and simplified:

$$\mathbf{T}_{inv} = \frac{1}{X_{base|x_p|}} \begin{bmatrix} x_{p\alpha}\frac{d}{dt}x_\alpha^q - x_{p\beta}\frac{d}{dt}x_\alpha & x_{p\alpha}\frac{d}{dt}x_\alpha + x_{p\beta}\frac{d}{dt}x_\alpha^q \\ x_{p\alpha}\frac{d}{dt}x_\beta^q - x_{p\beta}\frac{d}{dt}x_\beta & x_{p\alpha}\frac{d}{dt}x_\beta + x_{p\beta}\frac{d}{dt}x_\beta^q \end{bmatrix} \tag{56}$$

REFERENCES

[1] S. K. Chung, "Phase-locked loop for grid-connected three-phase power conversion systems," *IEE Proc. Elect. Power Appl.*, vol. 147, no. 3, pp. 213–219, May 2000.

[2] J. L. Duarte, A. Van Zwam, C. Wijnands, and A. Vandenput, "Reference frames fit for controlling PWM rectifiers," *IEEE Trans. Ind. Electron.*, vol. 46, no. 3, pp. 628–630, Jun. 1999.

[3] M. Malinowski, M. P. Kazmierkowski, S. Hansen, F. Blaabjerg, and G. D. Marques, "Virtual flux based direct power control of three-phase PWM rectifier," *IEEE Trans. Ind. Appl.*, vol. 37, no. 4, pp. 1019–1027, Jul./Aug. 2001.

[4] P. Rioual, H. Pouliquen, and J.-P. Louis, "Regulation of a PWM rectifier in the unbalanced network state using a generalized model," *IEEE Trans. Power Electron.*, vol. 11, no. 3, pp. 495–502, May 1996.

[5] A. G. Yepes, A. Vidal, O. López, and J. Doval-Gandoy, "Evaluation of techniques for cross-coupling decoupling between orthogonal axes in double synchronous reference frame current control," *IEEE Trans. Ind. Electron.*, vol. 61, no. 7, pp. 3527–3531, Jul. 2014.

[6] Y. Sato, T. Ishizuka, K. Nezu, and T. Kataoka, "A new control strategy for voltage-type PWM rectifiers to realize zero steady-state control error in input current," *IEEE Trans. Ind. Appl.*, vol. 34, no. 3, pp. 480–486, May/Jun. 1998.

[7] D. Roiu, R. I. Bojoi, L. R. Limongi, and A. Tenconi, "New stationary frame control scheme for three-phase PWM rectifiers under unbalanced voltage dips conditions," *IEEE Trans. Ind. Appl.*, vol. 46, no. 1, pp. 268–277, Jan./Feb. 2010.

[8] Z. Li, Y. Li, P. Wang, H. Zhu, C. Liu, and W. Xu, "Control of three-phase boost-type PWM rectifier in stationary frame under unbalanced input voltage," *IEEE Trans. Power Electron.*, vol. 25, no. 10, pp. 2521–2530, Oct. 2010.

[9] F. Wang, J. L. Duarte, and M. A. M. Hendrix, "Pliant active and reactive power control for grid-interactive converters under unbalanced voltage dips," *IEEE Trans. Power Electron.*, vol. 26, no. 5, pp. 1511–1521, May 2011.

[10] W. Jiang, Y. Wang, J. Wang, L. Wang, and H. Huang, "Maximizing instantaneous active power capability for PWM rectifier under unbalanced grid voltage dips considering the limitation of phase current," *IEEE Trans. Ind. Electron.*, vol. 63, no. 10, pp. 5998–6009, Oct. 2016.

[11] A. Camacho, M. Castilla, J. Miret, A. Borrell, and L. G. de Vicuña, "Active and reactive power strategies with peak current limitation for distributed generation inverters during unbalanced grid faults," *IEEE Trans. Ind. Electron.*, vol. 62, no. 3, pp. 1515–1525, Mar. 2015.

[12] G. Iwanski, "Virtual torque and power control of a three-phase converter connected to an unbalanced grid with consideration of converter current constraint and operation mode," *IEEE Trans. Power Electron.*, vol. 34, no. 4, pp. 3804–3818, Apr. 2019.

[13] Y. Zhang, J. Liu, H. Yang, and J. Gao, "Direct power control of pulse width modulated rectifiers without DC voltage oscillations under unbalanced grid conditions," *IEEE Trans. Ind. Electron.*, vol. 65, no. 10, pp. 7900–7910, Oct. 2018.

[14] H. Nian, Y. Shen, H. Yang, and Y. Quan, "Flexible grid connection technique of voltage-source inverter under unbalanced grid conditions based on direct power control," *IEEE Trans. Ind. Appl.*, vol. 51, no. 5, pp. 4041–4050, Sep./Oct. 2015.

[15] S. Wodyk and G. Iwanski, "Control of three-phase power electronic converter with power controllers in stationary frame," *IEEE Trans. Ind. Appl.*, vol. 56, no. 5, pp. 5257–5268, Sep./Oct. 2020.

[16] G. Iwanski, P. Maciejewski, and T. Łuszczyk, "New stationary frame transformation for control of a three-phase power converter under unbalanced grid voltage sags," *IEEE J. Emerg. Sel. Topics Power Electron.*, to be published, doi: 10.1109/JESTPE.2020.3012971.

[17] A. Fathi, Q. Shafiee, and H. Bevrani, "Robust frequency control of microgrids using an extended virtual synchronous generator," *IEEE Trans. Power Syst.*, vol. 33, no. 6, pp. 6289–6297, Nov. 2018.

[18] A. Camacho, M. Castilla, J. Miret, L. G. de Vicuña, and R. Guzman, "Positive and negative sequence control strategies to maximize the voltage support in resistive–inductive grids during grid faults," *IEEE Trans. Power Electron.*, vol. 33, no. 6, pp. 5362–5373, Jun. 2018.

[19] T. E. Nunez-Zuniga and J. A. Pomilio, "Shunt active power filter synthesizing resistive loads," *IEEE Trans. Power Electron.*, vol. 17, no. 2, pp. 273–278, Mar. 2002.

[20] S. Castellan, G. Buja, and R. Menis, "Single-phase power line conditioning with unity power factor under distorted utility voltage," *Int. J. Elect. Power Energy Syst.*, vol. 121, Oct. 2020, Art. no. 106057.

[21] P. Xiao, K. A. Corzine, and G. K. Venayagamoorthy, "Multiple reference frame-based control of three-phase PWM boost rectifiers under unbalanced and distorted input conditions," *IEEE Trans. Power Electron.*, vol. 23, no. 4, pp. 2006–2017, Jul. 2008.

[22] A. Galecki, M. Michalczuk, A. Kaszewski, B. Ufnalski, and L. Grzesiak, "Particle swarm optimization of the multioscillatory LQR for a three-phase grid-tie converter," *Przeglad Elektrotechniczny*, vol. 94, no. 6, pp. 43–48, 2018.

[23] Z. Xin, X. Wang, Z. Qin, M. Lu, P. C. Loh, and F. Blaabjerg, "An improved second-order generalized integrator based quadrature signal generator," *IEEE Trans. Power Electron.*, vol. 31, no. 12, pp. 8068–8073, Dec. 2016.

Sebastian Wodyk received the M.Sc. degree in electrical engineering in 2018 from the Faculty of Electrical Engineering, Warsaw University of Technology, Warszawa, Poland, where he has been working toward the Ph.D. degree in automation and robotics since 2018.

His research interests include control systems of grid-connected power converters and electrical energy storage systems for renewable energy sources and electrical vehicles.

Grzegorz Iwanski (Senior Member, IEEE) received the M.Sc. degree in automatic control and robotics and the Ph.D. degree in electrical engineering from the Faculty of Electrical Engineering, Warsaw University of Technology (WUT), Warsaw, Poland, in 2003 and 2005, respectively.

From 2006 to 2008, he was a Research Worker involved in an international project within the Sixth Framework Program of the European Union. Since 2009, he has been an Assistant Professor with the Institute of Control and Industrial Electronics, WUT, where he became an Associate Professor in 2019. From 2012 to 2013, he joined the Renewable Electrical Energy System Team, Universitat Politècnica de Catalunya, Barcelona, Spain, within the framework of the scholarship of Polish Minister of Science and Higher Education. He teaches courses on power electronics, drives, and power conversion systems. He is a coauthor of one monograph, three book chapters, and about 80 journal articles and conference papers. His research interests include variable and adjustable speed power generation systems, photovoltaics and energy storage systems, and automotive power electronics and drives.

Dr. Iwanski provided two plenary lectures on IEEE technically sponsored international conferences: Ecological Vehicles and Renewable Energies in 2015 and Joint International Conference on Optimization of Electrical and Electronic Equipment and Aegean Conference on Electrical Machines and Power in 2017.